



Experimental investigation of dry feed operation in a polymer electrolyte membrane fuel cell

P.K. Jithesh, T. Sundararajan, Sarit K. Das*

Department of Mechanical Engineering, Indian Institute of Technology Madras, Chennai 600 036, India



HIGHLIGHTS

- Product water is used to hydrate the polymer electrolyte membrane.
- Non-uniform under-rib convection in the mixed distributor aids to retain water.
- Voltage depends on operating temperature and stoichiometry in co-flow mode.
- Voltage independent of operating temperature and stoichiometry in counter-flow mode.
- Horizontal orientation of the flow field is ideal for self-humidified operation.

ARTICLE INFO

Article history:

Received 12 January 2014

Received in revised form

26 February 2014

Accepted 1 March 2014

Available online 12 March 2014

Keywords:

Polymer electrolyte membrane fuel cell

Water management

Self-humidification

Under-rib convection

ABSTRACT

The possibility of achieving self-humidified operation of a polymer electrolyte membrane fuel cell, without any major modifications to the conventional fuel cell design, is investigated experimentally. The flow distributor is designed such that the non-uniform under-rib convection aids to retain product water in the fuel cell enabling a dry feed operation. The fuel cell is operated in a pseudo co-flow and pseudo counter flow modes at a constant current density and the transient change in voltage and temperature are recorded. In the pseudo co-flow mode, the voltage drops at higher temperature and reactant stoichiometries which is attributed to membrane dehydration at the inlet region of the cell. In the pseudo counter-flow mode, the voltage remains same at both low and high temperature operation and is found to be independent of reactant stoichiometry. A horizontal orientation of the flow field, in pseudo counter flow mode, is found to be ideal for self-humidified operation at low reactant stoichiometries and cell temperature.

© 2014 Elsevier B.V. All rights reserved.

1. Introduction

Water management is one of the important challenges that needs to be addressed to make polymer electrolyte membrane (PEM) fuel cells a commercially viable product. In water management, the supply, generation and removal of water is balanced in such a way that the electrolyte membrane is always well hydrated. The proton conductivity of the electrolyte membrane increases with the water content in it [1], and thus ensuring a well hydrated membrane is essential to get maximum performance from the fuel cell [2,3].

Conventionally, external humidification systems are provided to humidify the reactant gases before entering the cell so that

sufficient water is available to hydrate the membrane. In self-humidification approach, the water generated in the fuel cell itself is used to humidify the reactants and hydrate the membrane. Excess water, if not removed effectively, will hinder reactant transport through the gas diffusion layer and will also reduce the active area available for reaction [4]. Hence, the reactant flow is maintained at a sufficiently high rate to flush out the excess water.

Self-humidification eliminates the complexity, cost, weight and parasitic power loss associated with an external humidification system. Büshi and Srinivasan [5] showed through experiments that with suitable choice of operating conditions self-humidification of PEM fuel cells are possible. The performance of a self-humidified PEM fuel cell depends on the operating temperature, pressure and reactant flow rate as these factors directly affect the amount of water generated and carried away from the fuel cell [6–9]. High operating temperature is critical in deciding the fuel cell performance as it has a negative impact on water retention but favors

* Corresponding author. Tel.: +91 44 22574655; fax: +91 44 22570545.

E-mail addresses: skdas@iitm.ac.in, sarit_das@hotmail.com (S.K. Das).

reaction kinetics. Depending on the level of membrane hydration, multiple steady states of current and voltage can occur at same operating conditions [10]. In another important work, Feindel et al. [11] experimentally observed the formation and distribution of liquid water on cathode side and its effect on the performance of a self-humidified PEM fuel cell.

There are many interesting studies in literature on achieving self-humidification in PEM fuel cells. In one of the earlier works Watanabe et al. [12], proposed using a thin electrolyte membrane impregnated with small amounts of platinum catalyst to benefit from oxidation of cross-over hydrogen and subsequent adsorption of the generated water with a hygroscopic material. A novel method for preparing such self-humidifying membranes is given by Yang et al. [13]. Ge et al. [14] presented an experimental study in which, two strips of wick made of polyvinyl alcohol sponge is mounted to the flow distributor plate to retain product water and humidify the cathode stream.

Tolj et al. [15] achieved internal humidification by employing spatially variable heat removal rates to maintain the relative humidity of cathode stream near the saturated state from cell inlet to outlet. Other important works include using a porous carbon flow field plate on the cathode side to benefit from the capillary distribution of water [16], adding silica to the catalyst layer on the anode side to retain water and humidify the membrane [17,18] and recirculating the cathode exhaust gas to replace the external humidification system [19].

Qi and Kaufman [20] investigated dry feed operation of a PEM fuel cell stack with a double-path-type counter-current flow field. A stable operation of the stack is obtained as the flow arrangement is found to provide better hydration of the membrane and even distribution of reactants. The effect of flow field design, flow field combination and flow direction in a PEM fuel cell stack for portable applications is investigated by Tüber et al. [21]. The experiments showed that a meander flow field with outwards-vectored flow direction exhibits better performance. The effect of flow direction on self-humidification in PEM fuel cells is numerically investigated using a two dimensional, steady state model by Ge and Yi [22]. The simulations showed that a counter flow mode of operation gives high performance and proper humidification as well as better current density distribution with dry or low humidity reactant gases, compared to a co-flow mode of operation.

From the literature it can be seen that most of the works on self-humidification in PEM fuel cells either requires a modification to the materials used or to the system itself. In the present study, self-humidification is achieved by employing a mixed flow distributor, which due to its inherent flow maldistribution and non-uniform under-rib convection, retains product water in the cell. This flow distributor is selected based on our previous computational study on liquid water distribution characteristics of different type of flow distributors [23]. The study showed that a mixed flow distributor exhibits more uniform liquid water distribution from cell inlet to outlet. The objective of the present study is to investigate the possibility of using a mixed flow distributor to achieve self-humidified operation of a conventional PEM fuel cell, without any additional modifications to the system or components.

2. Experimental section

The experiments are conducted on a PEM fuel cell of 25 cm^2 active area. The membrane electrode assembly (Dura-MEA®5Pt5L25) consists of Nafion NR-212 membrane as the electrolyte and Ballard carbon paper (MGL 370) as gas diffusion layer. The catalyst layers has a platinum loading of 0.5 mg cm^{-2} on the cathode side and 0.25 mg cm^{-2} on the anode side. The flow field is machined on graphite plates of 10 mm thickness. The end plates are

made of stainless steel, since the low thermal conductivity of the material reduces heat loss to the surroundings.

To regulate the reactant flow rate, a mass flow controller (Aalborg®-GFC17) is used for hydrogen and a rotameter is used for oxygen. The rotameter is used so as to purge the cathode side easily whenever the voltage drops due to liquid water accumulation in the cell. A data acquisition unit (Agilent-34970A) is used to record the transient change in cell voltage and temperature. The temperature of the cell is measured using a J-type thermocouple. The accuracy of voltage measurement is $\pm 80\text{ }\mu\text{V}$ and that of temperature is $\pm 1.1\text{ }^\circ\text{C}$. An electronic load box (K-Pas Instronic Engineers India Private Ltd) is used to apply electrical load to the fuel cell.

2.1. Mixed flow distributor

A schematic of the mixed flow field used in the present study is shown in Fig. 1. The mixed flow distributor exhibits better water distribution characteristics compared to a parallel or serpentine distributor [23]. The distributor is similar to the series-parallel design employed in the self-humidification experiments by Büshi and Srinivasan [5] and Ge et al. [14].

It is well known that in flow distributors used in PEM fuel cells, the pressure difference between adjacent channels induce an under-rib convection or cross flow of reactants through the porous gas diffusion layer. Under-rib convection aids to bring in fresh reactants to the active area below ribs and also flushes out product water from these regions, thus enhancing the performance of the fuel cell [24].

The advantage of a mixed flow distributor is that, the rate of under-rib convection will be different below each rib due to the flow maldistribution in the header. For example, in the present configuration, when flow is getting divided in to three channels from the common header, the third channel ch3 (see Fig. 1) in the flow sector, will receive higher flow rate due to high momentum in $-Y$ direction and channel ch1 will receive less flow rate. This results in a high rate of under-rib convection below rib rb3, and a low rate of under-rib convection below rib rb1. Hence, more water will be removed from region below rb3 whereas water removal will be less in region below rib rb1. Additionally, as under-rib convection is strong at the inlet of the channel and becomes weak towards

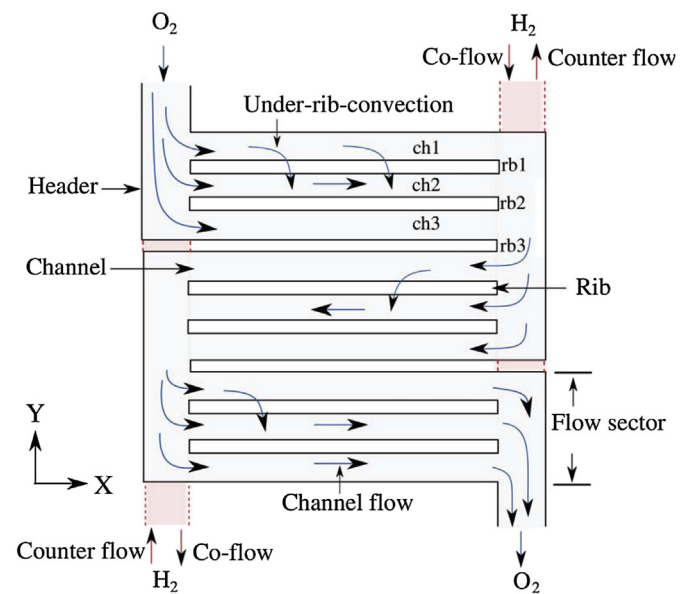


Fig. 1. Schematic of the mixed flow distributor showing the co-flow and counter-flow modes of operation.

the outlet of the channel, more water will be retained towards the end region of the ribs. This phenomenon of non-uniform under-rib convection helps to retain some water to hydrate the membrane and simultaneously remove the excess to reduce chances of flooding. In the present design, the flow gets distributed into three parallel channels from the header and this is expected to retain more water in the cell compared to flow getting split into two channels as we considered in the previous study [23].

The same flow field design is used on both anode and cathode sides. There are seven flow sectors in the flow field each consisting of three parallel channels of 50 mm length, 1.5 mm width and 1 mm depth. The ribs separating the channels are 1.0 mm wide.

2.2. Methodology

The fuel cell is fed with dry oxygen and hydrogen on the cathode and anode sides respectively. The reactants enter the cell at ambient temperature and at a pressure of 1 atm gauge. The fuel cell is operated at a constant current density and the transient change in cell voltage and temperature are monitored till a steady state is reached. The voltage is measured between the anode and cathode flow distributor plates and the temperature is measured on the cathode flow distributor plate.

The reactants are fed either in a pseudo co-flow or in a pseudo counter-flow mode as shown in Fig. 1. In the pseudo co-flow mode oxygen and hydrogen enters at the top of the cell and in the pseudo counter-flow mode hydrogen flows from bottom to top. It may be noted that, the reactant flow in the anode and cathode channels on both sides of the membrane electrode assembly are in the opposite direction in pseudo co-flow mode and are in the same direction in pseudo counter-flow mode.

No external heating system is used in the present study to maintain the temperature of the fuel cell, but the operating temperature increases due to the heat of reaction. The final steady state temperature is attained when the sum total of heat loss by natural convection from the fuel cell and the heat carried away by the excess reactant feed is equal to the heat generated in the electrochemical reaction. This approach is taken to get better insights to the performance of the fuel cell at varying temperatures.

3. Results and discussions

The self-humidification characteristics of the PEM fuel cell under study are investigated by varying the reactant stoichiometries and flow direction. The results are discussed below.

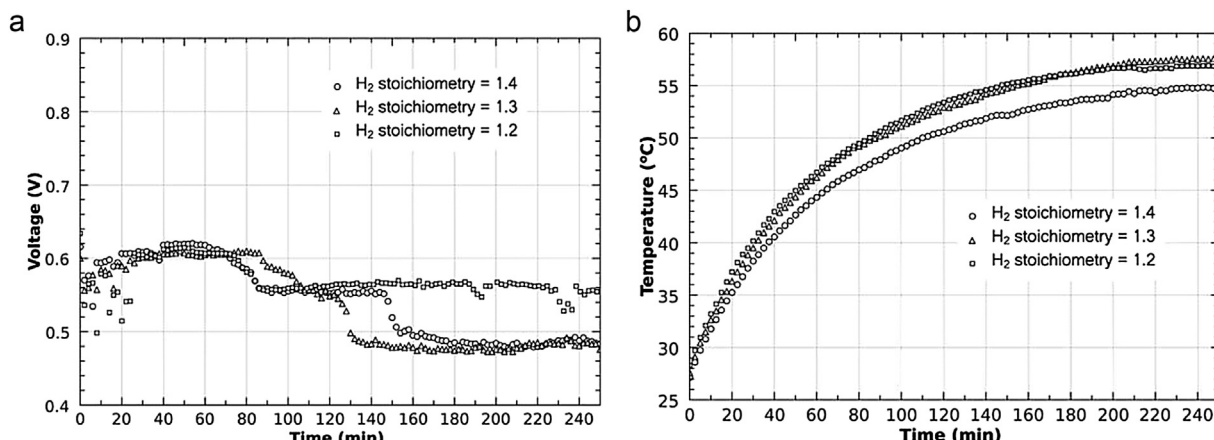


Fig. 2. Effect of hydrogen stoichiometry on performance in co-flow mode of operation (a) variation of cell voltage with time (b) variation of cell temperature with time ($i = 0.8 \text{ A cm}^{-2}$, $\xi_{O_2} = 3.3$).

3.1. Effect of hydrogen stoichiometry: pseudo co-flow mode

The variation in cell voltage at a constant current density of 0.8 A cm^{-2} and oxygen stoichiometry of 3.3 is shown in Fig. 2a. The hydrogen stoichiometries are 1.2, 1.3 and 1.4. The corresponding transient change in cell temperature is shown in Fig. 2b. The fuel cell is at ambient temperature when the load is applied and as a result product water will be in liquid form inside the fuel cell. The voltage is found to drop frequently due to liquid water accumulation and the cathode side is purged several times to remove the excess liquid water and to improve the voltage. The voltage is stabilized after 35 min of operation when the cell temperature reaches around 40°C . At this stage membrane is well hydrated and the fuel cell performance is steady.

It can be seen from Fig. 2 that at low temperatures, the cell voltage is above 0.6 V but as cell temperature increases to 50°C the voltage drops to 0.56 V. For hydrogen stoichiometries of 1.3 and 1.4, the voltage further drops to 0.48 V with increase in temperature. This second drop in voltage is not observed when the hydrogen stoichiometry is 1.2.

This variation in voltage can be attributed to the change in equilibrium between different water transport mechanisms across the electrolyte membrane due to the increase in temperature. At low temperatures, more liquid water will be present on the cathode side and the concentration gradient drives a water flux to the anode side through the membrane. This diffusion flux will dominate the electro-osmotic drag of water from anode to cathode and thus the membrane will be well hydrated. The high voltage at low temperature is an indication of the low Ohmic resistance of the membrane.

As cell temperature increases, the saturation pressure of water vapor increases and the product water starts to evaporate. The dry oxygen entering the cathode side effectively removes this water vapor formed by evaporation. This increase in water removal by cathode stream reduces the back diffusion to the anode side and the membrane water content decreases resulting in an increase in proton transport resistance and a drop in voltage.

As the temperature increases further, water starts to evaporate on the anode side also. This increases the water removed by the anode stream and results in further reduction in membrane water content and subsequent drop in voltage. This second drop in voltage can be seen in the case of hydrogen stoichiometries 1.3 and 1.4 but is not observed for the hydrogen stoichiometry of 1.2. Higher reactant stoichiometries favor the removal of water from the fuel cell leading to reduction in water content in the membrane and subsequent performance loss [9]. At lower stoichiometries less

water is removed thus increasing the hydration of the membrane and proton conductivity.

The drop in voltage can also be explained by the idea of progressing drying front proposed by Sanchez and Garcia-Ybarra [25]. As the temperature increases, the dehydration of the membrane starts at the reactant inlet region, since the dry feed takes up the evaporated water. The rate of electro-chemical reaction remains same since current is kept constant but the active area shifts to regions where membrane is well hydrated. This reduction in active area results in the first drop in voltage. The dry front further propagates away from the inlet region as the cell temperature and evaporative water removal increases. The voltage again starts to drop due to dehydration of membrane and shifting of active area and then stabilizes at a constant value. There is no further drop in voltage as the cell temperature reaches a steady state and the drying front ceases to propagate. In another experimental study, Owejan et al. [26] showed through neutron radiograph images of water distribution and high-frequency resistance measurements that, the movement of drying front during dry air purge causes an increase in cell resistance. Although the results presented are for a shutdown purge sequence, the evaporative removal of water and subsequent membrane dehydration observed, supports the interpretation that the voltage drop observed at higher temperatures in the present study, is due to membrane dehydration.

From Fig. 2b it can be seen that, after 240 min of operation, the cell temperature reaches a steady state and the voltage continues to remain at the stabilized value for different stoichiometries. The steady state temperature is 55 °C for the hydrogen stoichiometry of 1.4 which is slightly lower than the other two cases. This is only an effect of a low ambient temperature, as the cooling of the fuel cell in the present study is mainly by natural convection. To verify this we repeated the experiment with the same reactant stoichiometries on a day with higher ambient temperature and the comparison is shown in Fig. 3. During the course of experiment, the ambient temperature is found to vary from 27 to 30 °C in case-1 and from 30 to 33 °C in case-2. The final stabilized voltage is found to be 0.48 V in both the cases. From the transient temperature data it can be confirmed that the final steady state temperature of the fuel cell depends mainly on the ambient temperature for the present design of experiments.

Another important feature regarding the drop in voltage can be observed from Fig. 3a. In the case 2, the first and second drop in voltage is delayed compared to case 1, but the final stabilized voltages are same. This is due to the different levels of membrane hydration, as the membrane hydration depends on

the number of times the cathode is purged, which is different in both cases.

It may be noted that, cathode purging is done manually and only when a significant drop in voltage is observed. For example, as can be seen from Fig. 2a, for a hydrogen stoichiometry of 1.2, cathode purging is performed at 195 min and 235 min when a drop in voltage is observed and this brought back the voltage to original stabilized value. The number of purging performed during the first 30 min of operation is different in all the experiments and this might influence the membrane hydration. Purging is found to have no effect on performance once the voltage is stabilized.

3.2. Effect of oxygen stoichiometry: pseudo co-flow mode

The transient voltage and temperature data for a pseudo co-flow mode operation of the fuel cell with two different oxygen stoichiometries (3.3 and 2.7) are shown in Fig. 4a and b respectively. The hydrogen stoichiometry is maintained at 1.2 since it is found to give a higher voltage at high cell temperatures.

In both the cases voltage is found to drop as temperature increases, but in the case of stoichiometry 2.7 the drop is delayed compared to the higher stoichiometry of 3.3. This delay can be attributed to better membrane hydration as a result of reduced water removal from the cell since the reactant flow rate is low. Dehydration of the membrane at higher oxygen flow rates and increase in water content in the membrane at lower oxygen flow rates is also observed in the ¹H NMR microscopy images by Feindel et al. [11].

The stabilized voltage at low and high temperatures is found to be 0.62 and 0.56 respectively in both the cases. The second drop in voltage observed in the higher hydrogen stoichiometry operation is not seen here as the hydrogen stoichiometry is kept low. The corresponding transient temperature data for these cases is shown in Fig. 4b. The cell temperature is found to be steady at 57 °C.

We also operated the cell with a lower oxygen stoichiometry of 2.0, to see whether the drop in voltage at higher temperatures is delayed further. In this case, however, the performance is found to be unstable at both low and high temperature operation as the reduced rate of water removal lead to liquid water accumulation in the cell. This implies that oxygen stoichiometry should be sufficiently high to remove excess water even when the self-humidification method is used.

In practical applications, air at a higher stoichiometry is used in PEM fuel cells. At higher air flow rates, product water removal and

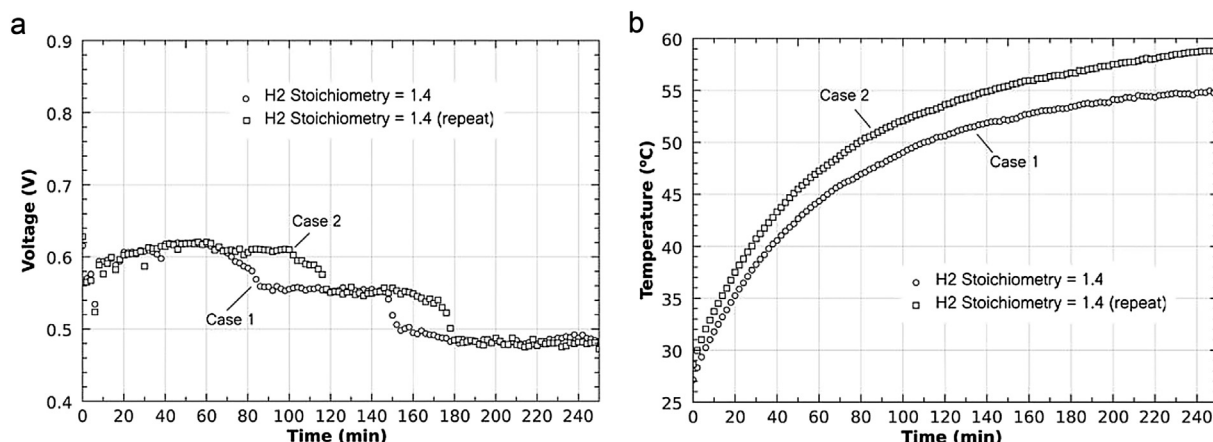


Fig. 3. Effect of initial membrane hydration on performance in co-flow mode of operation (a) Variation of cell voltage with time (b) variation of cell temperature with time ($i = 0.8 \text{ A cm}^{-2}$, $\xi_{H_2} = 1.4$, $\xi_{O_2} = 3.3$).

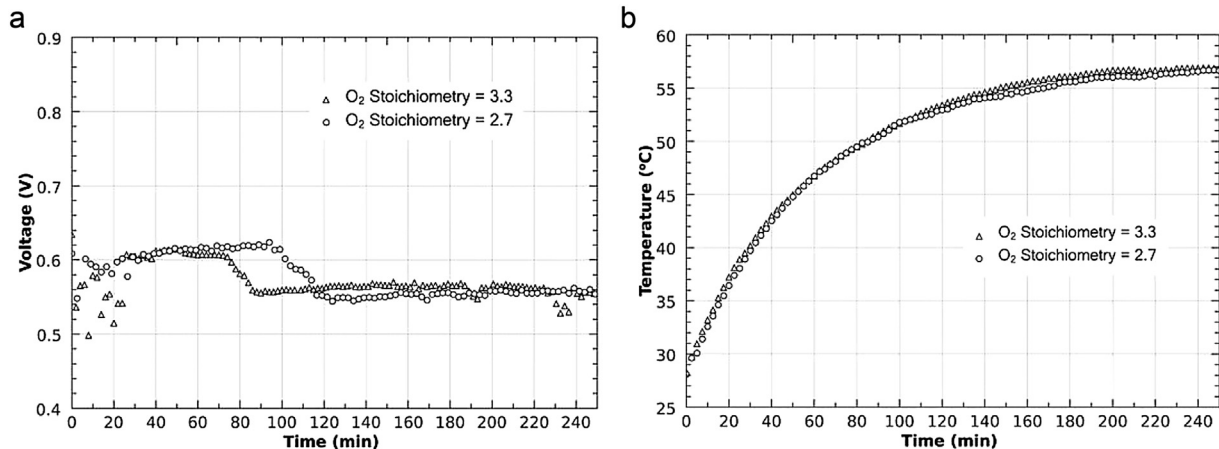


Fig. 4. Effect of oxygen stoichiometry on performance in co-flow mode of operation (a) variation of cell voltage with time (b) variation of cell temperature with time ($i = 0.8 \text{ A cm}^{-2}$, $\xi_{\text{H}_2} = 1.2$, $\xi_{\text{O}_2} = 2.7, 3.3$).

membrane dehydration will be more and the fuel cell performance will reduce. It is found from a computational study (not reported here) that, if the number of parallel channels in each flow sector of the mixed flow distributor is increased, then even at higher flow rates water is retained in the fuel cell. Hence, for air operation, a mixed flow distributor with 4 or 5 channels in each flow sector could be employed. The results are also relevant to applications where the PEM fuel cell is directly fed with ambient air, with no control over inlet relative humidity or temperature.

3.3. Effect of flow direction: pseudo co-flow and pseudo counter-flow modes

In this section the self-humidification characteristics of the fuel cell in the pseudo co-flow and pseudo counter-flow modes are compared. The hydrogen and oxygen stoichiometry are 1.2 and 2.7 respectively and the current density is set at 0.8 A cm^{-2} . A comparison of the transient voltage and temperature data in both modes of operation are shown in Fig. 5a and b respectively.

In the pseudo counter-flow mode operation, the voltage is found to be same at lower as well as higher temperatures. This is a significant difference compared to the pseudo co-flow mode operation in which case a drop in voltage is observed at higher temperatures.

In the pseudo co-flow mode operation dry oxygen and hydrogen enters at top of the cell and hence there is no proper hydration of the membrane in this region. At lower temperatures, the rate of evaporation and thus the rate of water removal by reactant stream will be less and as a result more water is retained in the cell and the membrane gets well hydrated. At higher temperatures more water is removed by the reactant stream resulting the membrane dehydration and performance drop.

In the pseudo counter-flow mode, oxygen enters at top and hydrogen enters at bottom of the cell. The water content in cathode stream increases from inlet to outlet as more product water is evaporated. Simultaneously, the partial pressure of oxygen reduces due to consumption for reaction. The resulting increase in the partial pressure of water vapor towards the cathode outlet creates a concentration gradient of water from cathode to anode side which drives water diffusion flux through the membrane. The membrane thus gets well hydrated towards the cathode outlet.

The hydrogen entering the bottom of the cell gets humidified by the water that is diffused to anode side and transports it to the top of the cell. Again the partial pressure of hydrogen in the anode stream reduces from inlet to outlet due to consumption of hydrogen for reaction whereas the partial pressure of water vapor increases. The concentration gradient developed as a result of higher water content towards the anode outlet and lower water

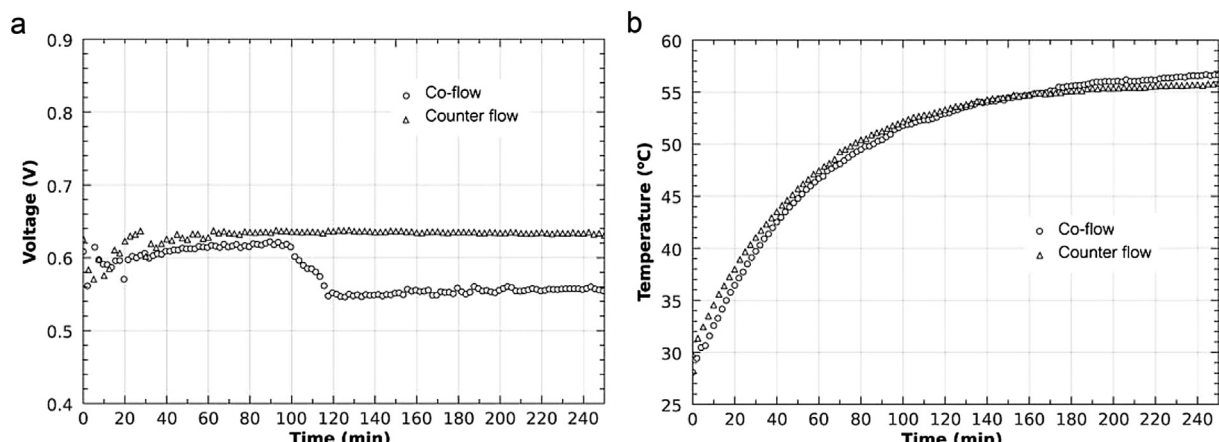


Fig. 5. Comparison of co-flow and counter-flow modes of operation (a) variation of cell voltage with time (b) variation of cell temperature with time ($i = 0.8 \text{ A cm}^{-2}$, $\xi_{\text{H}_2} = 1.2$, $\xi_{\text{O}_2} = 2.7$).

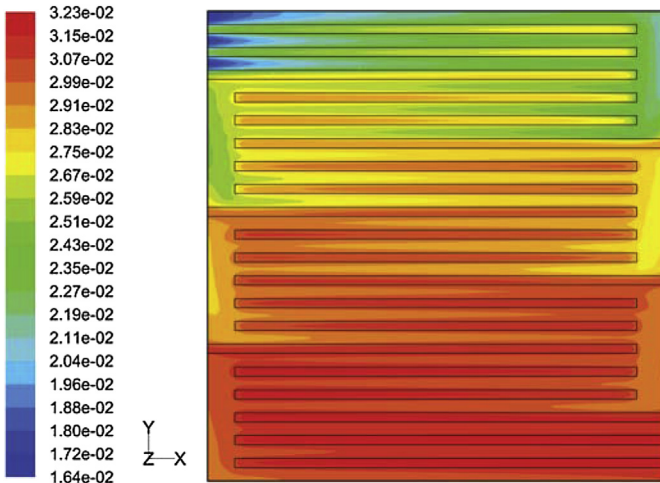


Fig. 6. Concentration of water vapor (kmol m^{-3}) in the cathode catalyst layer ($i = 0.75 \text{ A cm}^{-2}$, $\xi_{\text{O}_2} = 2.7$, $T_{\text{In},\text{O}_2} = 30^\circ\text{C}$, $T_{\text{In},\text{O}_2} = 30^\circ\text{C}$, $T_{\text{cell}} = 57^\circ\text{C}$).

content on the cathode inlet region across the membrane induces a back diffusion to the cathode side, resulting in better membrane hydration at the top region as well. In this way a consistent performance is observed from low to higher temperatures when the cell is operated in the pseudo counter-flow mode.

This explanation for the variation in performance due to the flow arrangement and its attribution to the water transport is consistent with the observation of Feindel et al. [11] on liquid water distribution in co-flow and counter flow modes of operation of a self-humidified PEM fuel cell and also agrees with the water diffusion model proposed in Ref. [5].

The concentration of water vapor in the catalyst layer obtained from a computational simulation of the cathode side of the fuel cell is shown in Fig. 6. The simulations are carried out using a three dimensional, steady state, non-isothermal numerical model considering the phase change of water. The details of the model and simulation techniques are given in our previous study [23]. It can be seen that, the concentration of water vapor is less at the inlet region of the cell, but increases towards the outlet. This supports the explanation of the experimental results that, while operating in a pseudo co-flow mode, at the inlet region of the cell membrane may not be well hydrated but towards the outlet diffusion of water from cathode to anode aids to hydrate the membrane. When operated in pseudo counter-flow mode, the hydrogen gets humidified by the diffused water and this humidified hydrogen hydrates the membrane at the top portion of the cell as well.

The effect of under-rib convection in a mixed flow distributor on the rate of water removal can also be identified from the simulated

distribution of water vapor. The concentration of water vapor is less at the beginning of each rib as under-rib convection is strong in this region but increases towards the end of the ribs as under-rib convection becomes weak. The water retained under each rib is also different. This phenomenon of non-uniform water removal is what makes the mixed flow distributor an ideal choice for flow distribution in self-humidified PEM fuel cells.

3.4. A discussion on the orientation of the flow field

In the self-humidification experiments by Büshi and Srinivasan [5], it is reported that there is not much change in performance when the fuel cell is operated in pseudo co-flow or pseudo counter-flow modes. With a similar flow field, however, we observed a significant difference in performance in the pseudo co-flow and pseudo counter-flow modes of operation. This difference can be attributed to the orientation of flow field inside the fuel cell. It can be oriented vertically such that the reactant flow in the channels is in the Y-direction (Fig. 7a) or can be oriented horizontally such that the channel flow is in the X-direction (Fig. 7b). From the schematic diagram provided in Ref. [5], it would appear that the flow field is placed in a vertical orientation. In this orientation there will be very less difference in pseudo co-flow or pseudo counter-flow modes of operation as in both cases membrane will be properly hydrated.

Ge et al. [14] also placed the flow field in a vertical orientation, but observed better performance in pseudo counter flow mode of operation. In their study, in pseudo counter-flow mode of operation air enters at point A (Fig. 7c) and hydrogen enters at point H, and in pseudo co-flow mode air and hydrogen enters at points A and E respectively. In the experiments by Büshi and Srinivasan [5], the reactant inlets are at points A and G in the pseudo counter-flow mode and at A and F in the pseudo co-flow mode. This comparison brings out the effect of the dry feed inlet/outlet location in the final assembly, on the performance of a self-humidified PEM fuel cell.

In the present study, based on our computational simulations, we have adopted a horizontal orientation of the flow field. In the pseudo co-flow mode hydrogen enters at E and leaves at H and in the pseudo counter-flow mode hydrogen enters at H and leaves at E. In both the modes, oxygen enters at A and leaves at D. In this arrangement product water removal is aided by gravity as oxygen is entering at the top of the cell. This is advantageous especially while operating at low temperatures as liquid water formation will be more.

We also operated the cell with a vertical orientation of flow field, but for the present operating conditions, the performance is found to be unstable due to poor liquid water removal. The same is observed when the flow field is oriented horizontally and oxygen inlet is provided at the bottom of the fuel cell (point D in Fig. 7c).

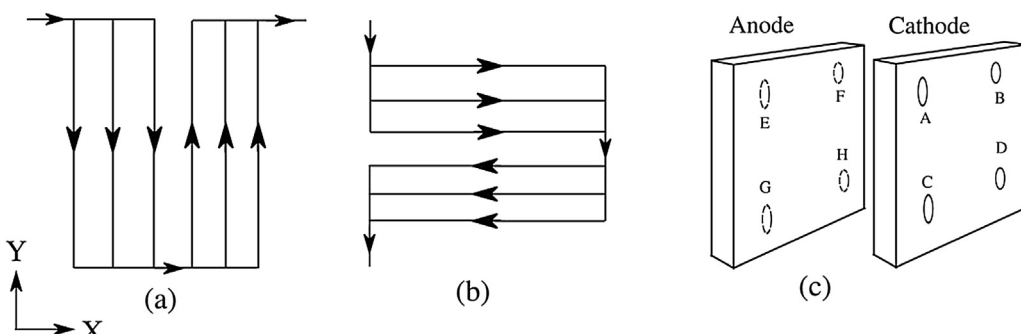


Fig. 7. (a) Vertical orientation (b) horizontal orientation (c) reactant inlet/outlet in cathode and anode end plates.

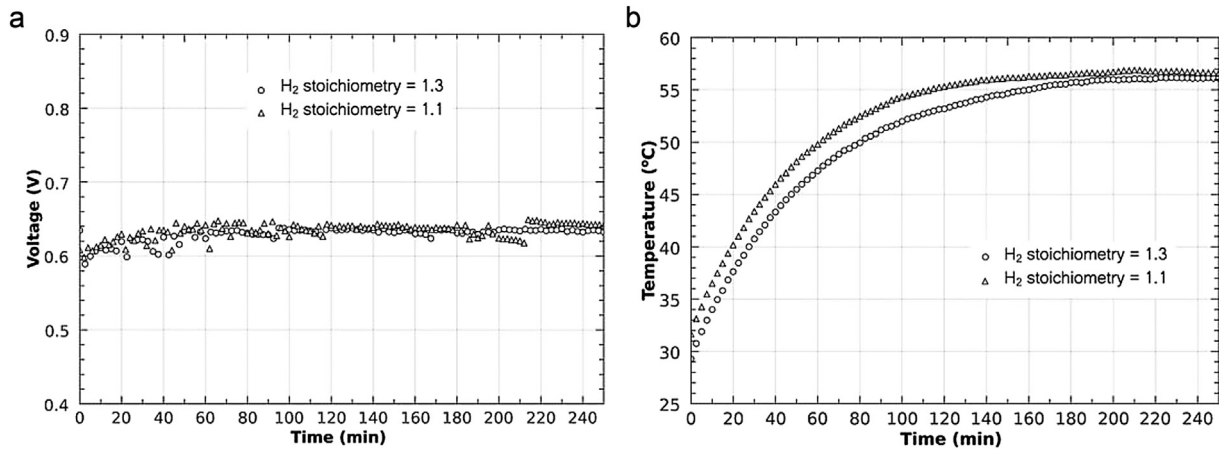


Fig. 8. Effect of hydrogen stoichiometry on performance in counter-flow mode of operation (a) variation of cell voltage with time (b) variation of cell temperature with time ($i = 0.8 \text{ A cm}^{-2}$, $\xi_{\text{H}_2} = 1.1, 1.3$, $\xi_{\text{O}_2} = 2.7$).

3.5. Effect of hydrogen stoichiometry: pseudo counter-flow mode

In the pseudo co-flow mode the hydrogen stoichiometry is found to have an effect on the stabilized voltage. In order to study the effect of stoichiometry in the pseudo counter flow mode, the fuel cell is operated at hydrogen stoichiometries of 1.1 and 1.3 and a current density of 0.8 A cm^{-2} . The cell voltage, shown in Fig. 8a, is found to remain same at both stoichiometries and is same as in the case of hydrogen stoichiometry 1.2. The cell temperature rises at a higher rate in the case of low stoichiometry operation as shown in Fig. 8b and can be attributed to reduced heat removal by hydrogen. In both the cases the final steady state temperature is found to be the same.

The performance of the cell is slightly better when operated at hydrogen stoichiometry of 1.1 especially at higher temperatures. This stoichiometry corresponds to a fuel utilization efficiency of 90.90%, which indicates that the self-humidified fuel cell can attain a higher energy conversion efficiency compared to externally humidified fuel cells.

3.6. Comparison with external humidification

The performance of the self-humidified fuel cell is compared with externally humidified condition in Fig. 9. The polarization

curve is drawn at constant reactant flow rate condition (water production and removal rates are different) when the cell temperature is at the steady state value of 57 °C. The voltage measured is across the copper current collector plates which is found to be 80–100 mV less than that measured across the flow distributor plates from low to high temperatures. In the external humidification experiment, the pseudo co-flow mode arrangement is used.

In the self-humidified pseudo co-flow mode operation, the voltage drop at higher current densities is found to be more compared to the other two cases. A maximum power density of 0.4 W cm^{-2} is observed at a current density of 0.83 A cm^{-2} . Hence, the analysis in the present study is carried out at current density of 0.8 A cm^{-2} . Self-humidification in the pseudo counter-flow mode gives comparable performance with externally humidified condition up to 0.7 A cm^{-2} . The subsequent deviation in performance can be attributed to membrane dehydration on the anode side due to increase in electro-osmotic drag.

4. Conclusions

The present experimental study investigates the effect of reactant stoichiometry and cell temperature on the performance of a self-humidified PEM fuel cell at different flow directions and flow field orientations. In the pseudo co-flow mode of operation, the cell voltage depends on reactant stoichiometry and cell temperature. At higher temperature and higher stoichiometries the voltage drops due to membrane dehydration. In the pseudo counter-flow mode the cell voltage is independent of reactant stoichiometry and cell temperature. The important conclusions drawn from the present study are:

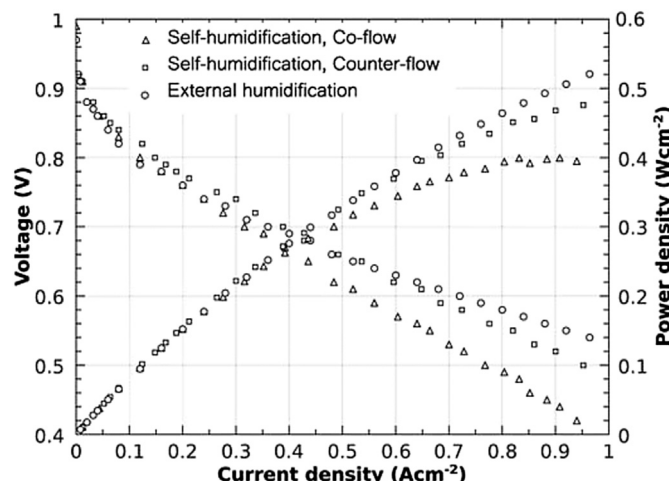


Fig. 9. Comparison of self-humidified and externally humidified operation ($\dot{V}_{\text{H}_2} = 170 \text{ sccm}$, $\dot{V}_{\text{O}_2} = 200 \text{ sccm}$, external humidification: $T_{\text{in},\text{O}_2} = T_{\text{in},\text{H}_2} = 60 \text{ }^{\circ}\text{C}$, $\Phi_a = \Phi_c = 100\%$, self-humidification: $T_{\text{in},\text{O}_2} = T_{\text{in},\text{H}_2} = 30 \text{ }^{\circ}\text{C}$).

1. A mixed flow distributor is a good choice for developing self-humidifying PEM fuel cells, without any additional modifications to the system, as it aids to retain product water inside the fuel cell.

2. A horizontal orientation of the flow field, with cathode stream entering at the top of the fuel cell, is ideal for preventing accumulation of product water especially at low temperature operation.

3. The present flow field arrangement and flow direction exhibits effective water removal even at lower reactant stoichiometries, thus providing a higher fuel utilization efficiencies and increase in overall energy conversion efficiency.

The findings from this study can be helpful in developing self-humidifying PEM fuel cells with better performance. As a future work the self-humidification performance of a PEM fuel cell stack with the mixed flow distributor is suggested.

Acknowledgment

The authors wish to thank Dr. G. Velayutham, Director, Sainergy Fuel Cell India Pvt Ltd for the helpful discussions in designing and fabricating the fuel cell.

Nomenclature

i	current density, (A cm^{-2})
T	temperature, ($^{\circ}\text{C}$)
\dot{V}	volume flow rate, (sccm)
ξ	stoichiometry
ϕ	relative humidity

References

- [1] T.E. Springer, T.A. Zawodzinski, S. Gottesfeld, *J. Electrochem. Soc.* 138 (1991) 2334–2342.
- [2] R. Eckl, W. Zehtner, C. Leu, U. Wagner, *J. Power Sources* 138 (2004) 137–144.
- [3] Y. Lee, B. Kim, Y. Kim, *Int. J. Hydrogen Energy* 34 (2009) 1999–2007.
- [4] S. Litster, C.R. Buie, J.G. Santiago, *Electrochim. Acta* 54 (2009) 6223–6233.
- [5] F.N. Büchi, S. Srinivasan, *J. Electrochem. Soc.* 144 (1997) 2767–2772.
- [6] M.V. Williams, H. Kunz, J.M. Fenton, *J. Power Sources* 135 (2004) 122–134.
- [7] Q. Dong, M.M. Mench, S. Cleghorn, U. Beuscher, *J. Electrochem. Soc.* 152 (2005) A2114–A2122.
- [8] W.H. Hogarth, J.B. Benziger, *J. Power Sources* 159 (2006) 968–978.
- [9] J. Zhang, Y. Tang, C. Song, X. Cheng, J. Zhang, H. Wang, *Electrochim. Acta* 52 (2007) 5095–5101.
- [10] W.H.J. Hogarth, J.B. Benziger, *J. Electrochem. Soc.* 153 (2006) A2139–A2146.
- [11] K.W. Feindel, S.H. Bergens, R.E. Wasylyshen, *J. Am. Chem. Soc.* 128 (2006) 14192–14199.
- [12] M. Watanabe, H. Uchida, Y. Seki, M. Emori, P. Stonehart, *J. Electrochem. Soc.* 143 (1996) 3847–3852.
- [13] T.-H. Yang, Y.-G. Yoon, C.-S. Kim, S.-H. Kwak, K.-H. Yoon, *J. Power Sources* 106 (2002) 328–332.
- [14] S. Ge, X. Li, I.-M. Hsing, *Electrochim. Acta* 50 (2005) 1909–1916.
- [15] I. Tolj, D. Bezmalinovic, F. Barbir, *Int. J. Hydrogen Energy* 36 (2011) 13105–13113.
- [16] S. Litster, J.G. Santiago, *J. Power Sources* 188 (2009) 82–88.
- [17] M. Han, S. Chan, S. Jiang, *Int. J. Hydrogen Energy* 32 (2007) 385–391.
- [18] H. Su, L. Xu, H. Zhu, Y. Wu, L. Yang, S. Liao, H. Song, Z. Liang, V. Birss, *Int. J. Hydrogen Energy* 35 (2010) 7874–7880.
- [19] B.J. Kim, M.S. Kim, *Int. J. Hydrogen Energy* 37 (2012) 4290–4299.
- [20] Z. Qi, A. Kaufman, *J. Power Sources* 109 (2002) 469–476.
- [21] K. Tüber, M. Zobel, H. Schmidt, C. Hebling, *J. Power Sources* 122 (2003) 1–8.
- [22] S.-H. Ge, B.-L. Yi, *J. Power Sources* 124 (2003) 1–11.
- [23] P.K. Jithesh, A.S. Bansode, T. Sundararajan, S.K. Das, *Int. J. Hydrogen Energy* 37 (2012) 17158–17171.
- [24] K.-S. Choi, B.-G. Kim, K. Park, H.-M. Kim, *Fuel Cells* 12 (2012) 908–938.
- [25] D. Sanchez, P. Garcia-Ybarra, *Int. J. Hydrogen Energy* 37 (2012) 7279–7288.
- [26] J.P. Owejan, J.J. Gagliardo, J.M. Sergi, S.G. Kandlikar, T.A. Trabold, *Int. J. Hydrogen Energy* 34 (2009) 3436–3444.